

# Large area resonant feedback random lasers based on dye-doped biopolymer films

Antonio Consoli,<sup>1,\*</sup> Danilo Mariano da Silva,<sup>2</sup> Niklaus Ursus Wetter,<sup>2</sup> and Cefe López<sup>1</sup>

<sup>1</sup>Instituto de Ciencia de Materiales de Madrid, Consejo Superior de Investigaciones Científicas, Calle Sor Juana Ines de la Cruz 3, 28049 Madrid, Spain

<sup>2</sup>Centro de Lasers e Aplicações, Instituto de Pesquisas Energéticas e Nucleares (CNEN-IPEN/SP), CEP 005508-000 São Paulo-SP, Brazil

\*antonio.consoli@csic.es

**Abstract:** We report resonant feedback random lasing from dye-doped biopolymer films, consisting of a deoxyribonucleic acid-cetyltrimethylammonium (DNA-CTMA) complex doped with DCM dye. In the proposed devices, the optical feedback for random lasing is given by scattering centers randomly positioned along the edges of the active area. Scattering elements are either titanium dioxide nanoparticles or random defects at the interface between active polymer and air. Different emission spectra are observed, depending on the geometry of the excited area. A single random resonator with dimensions of 2.6 mm x 0.65 mm is fabricated and random emission with resonant feedback is obtained by uniformly pumping the full device.

©2015 Optical Society of America

**OCIS codes:** (140.3380) Laser materials; (290.5880) Scattering, rough surfaces; (250.2080) Polymer active devices.

---

## References and links

1. D. S. Wiersma, "The physics and applications of random lasers," *Nat. Phys.* **4**(5), 359–367 (2008).
2. H. Cao, "Random lasers: development, features and applications," *Opt. Photonics News* **16**(1), 24–29 (2004).
3. B. Redding, M. A. Choma, and H. Cao, "Spatial coherence of random laser emission," *Opt. Lett.* **36**(17), 3404–3406 (2011).
4. B. Redding, M. A. Choma, and H. Cao, "Speckle-free laser imaging using random laser illumination," *Nat. Photonics* **6**(6), 355–359 (2012).
5. M. A. Noginov, *Solid-state random lasers* (Springer 2005), Chap. 10.
6. H. Cao, Y. G. Zhao, H. C. Ong, S. T. Ho, J. Y. Dai, J. Y. Wu, and R. P. H. Chang, "Ultraviolet lasing in resonators formed by scattering in semiconductor polycrystalline films," *Appl. Phys. Lett.* **73**(25), 3656–3658 (1998).
7. N. M. Lawandy, R. M. Balachandran, A. S. L. Gomes, and E. Sauvain, "Laser action in strongly scattering media," *Nature* **368**(6470), 436–438 (1994).
8. H. Cao, *et al.*, "Random lasers with coherent feedback," *IEEE J. Sel. Top. Quantum Electron.* **9**(1), 111–119 (2003).
9. M. Leonetti, C. Conti, and C. López, "Dynamics of phase-locking random lasers," *Phys. Rev. A* **88**(4), 043834 (2013).
10. M. Leonetti, C. Conti, and C. López, "The mode-locking transition of random lasers," *Nat. Photonics* **5**(10), 615–617 (2011).
11. S. K. Turitsyn, S. A. Babin, A. E. El-Taher, P. Harper, D. V. Churkin, S. I. Kablukov, J. D. Ania-Castañón, V. Karalekas, and E. V. Podivilov, "Random distributed feedback fibre laser," *Nat. Photonics* **4**(4), 231–235 (2010).
12. Q. Song, S. Xiao, Z. Xu, J. Liu, X. Sun, V. Drachev, V. M. Shalaev, O. Akkus, and Y. L. Kim, "Random lasing in bone tissue," *Opt. Lett.* **35**(9), 1425–1427 (2010).
13. G. Strangi, S. Ferjani, V. Barna, A. De Luca, C. Versace, N. Scaramuzza, and R. Bartolino, "Random lasing and weak localization of light in dye-doped nematic liquid crystals," *Opt. Express* **14**(17), 7737–7744 (2006).
14. L. Sznitko, J. Mysliwiec, and A. Miniewicz, "The role of polymers in random lasing," *J. Polym. Sci., B, Polym. Phys.* **53**(14), 951–974 (2015).
15. R. M. Balachandran, D. P. Pacheco, and N. M. Lawandy, "Laser action in polymeric gain media containing scattering particles," *Appl. Opt.* **35**(4), 640–643 (1996).
16. A. Tulek, R. C. Polson, and Z. V. Vardeny, "Naturally occurring resonators in random lasing of  $\pi$ -conjugated polymer films," *Nat. Phys.* **6**(4), 303–310 (2010).

17. Z. Yu, W. Li, J. A. Hagen, Y. Zhou, D. Klotzkin, J. G. Grote, and A. J. Steckl, "Photoluminescence and lasing from deoxyribonucleic acid (DNA) thin films doped with sulforhodamine," *Appl. Opt.* **46**(9), 1507–1513 (2007).
18. L. Sznitko, J. Mysliwiec, P. Karpinski, K. Palewska, K. Parafiniuk, S. Bartkiewicz, I. Rau, F. Kajzar, and A. Miniewicz, "Biopolymer based system doped with nonlinear optical dye as a medium for amplified spontaneous emission and lasing," *Appl. Phys. Lett.* **99**(3), 031107 (2011).
19. A. Camposeo, P. Del Carro, L. Persano, K. Cypriach, A. Szukalski, L. Sznitko, J. Mysliwiec, and D. Pisignano, "Physically transient photonics: random versus distributed feedback lasing based on nanoimprinted DNA," *ACS Nano* **8**(10), 10893–10898 (2014).
20. D. Wiersma, "Laser physics: The smallest random laser," *Nature* **406**(6792), 132–135 (2000).
21. J. Liu, P. D. Garcia, S. Ek, N. Gregersen, T. Suhr, M. Schubert, J. Mørk, S. Stobbe, and P. Lodahl, "Random nanolasing in the Anderson localized regime," *Nat. Nanotechnol.* **9**(4), 285–289 (2014).
22. R. V. Ambartsumyan, N. Basov, P. Kryukov, and V. S. Letokhov, "A laser with a nonresonant feedback," *IEEE J. Quantum Electron.* **2**(9), 442–446 (1966).
23. R. V. Ambartsumyan, N. Basov, P. Kryukov, and V. S. Letokhov, "Non-resonant feedback in lasers," *Prog. Quantum Electron.* **1**, 107 (1970).
24. M. Leonetti, R. Sapienza, M. Ibsate, C. Conti, and C. López, "Optical gain in DNA-DCM for lasing in photonic materials," *Opt. Lett.* **34**(24), 3764–3766 (2009).
25. L. Dal Negro, P. Bettotti, M. Cazzanelli, D. Pacifici, and L. Pavesi, "Applicability conditions and experimental analysis of the variable stripe length method for gain measurements," *Opt. Commun.* **229**(1-6), 337–348 (2004).
26. A. Vembris, E. Zarinsh, and V. Kokars, "Amplified spontaneous emission of glass forming DCM derivatives in PMMA films," *Proc. SPIE* **9137**, 91371E (2014).
27. E. M. Calzado, J. M. Villalvilla, P. G. Boj, J. A. Quintana, and M. A. Díaz-García, "Tuneability of amplified spontaneous emission through control of the thickness in organic-based waveguides," *J. Appl. Phys.* **97**(9), 093103 (2005).
28. A. K. Sheridan, G. A. Turnbull, A. N. Safonov, and I. D. W. Samuel, "Tuneability of amplified spontaneous emission through control of the waveguide-mode structure in conjugated polymer films," *Phys. Rev. B* **62**(18), R11929 (2000).
29. A. Tulek and Z. V. Vardeny, "Studies of random laser action in  $\pi$ -conjugated polymers," *J. Opt.* **12**(2), 024008 (2010).

---

## 1. Introduction

A random laser (RL) consists of a random distribution of scattering centers embedded in a material with optical gain [1,2]. Optical feedback is given by multiple scattering inside the active region, resulting in omnidirectional emission with high spectral and low spatial coherence [3]. This characteristic feature has found application in the first laser based speckle free imaging system [4] and is promising for display and lighting applications [5], as it combines the high energy conversion of lasers with omnidirectional emission and low spatial coherence.

Two emission regimes have been reported in RLs: (i) resonant feedback regime [6], characterized by a multi-mode spectrum with sub-nanometer linewidths and random lasing frequencies, and (ii) incoherent feedback regime (also known as intensity feedback) [7], consisting of a single-peaked broad (few nanometres) spectrum, originated from amplitude-only feedback, i.e. emission with no resonant optical cavity [8]. Recently, an alternative interpretation of incoherent emission has been given, associating the spectrum to a large number of modes that mutually couple together, resulting in a synchronized emission which recalls mode-locked behavior in classical lasers [9, 10].

Random lasing has been obtained in a wide range of materials, e.g. semiconductor powders [6], colloidal suspensions [7], optical fibers [11], biological tissues [12], liquid crystals [13] and polymers [14], demonstrating the ease of fabrication and flexibility in terms of required materials for these devices.

In polymer films, random lasing has been obtained by integrating scattering particles in the sample [15] or by taking advantage of the random local variation of the refractive index due to sample roughness and irregularity [16]. DNA based polymer films are a promising material choice for light amplification and lasing [17,18], both in conventional cavities and random resonators [19].

If, on one hand tight localization of light (in the Anderson regime) in RLs is appealing both theoretically and for practical applications [20,21], coherent random lasing emission on a

large area from a single device would be an advantage for lighting, display and imaging applications.

Lasing action in RLs is usually obtained with a spatially *distributed* feedback, where the scattering elements are embedded into the active material. Powders of semiconductors [6] and colloidal suspensions of scattering particles in a dye solution [7] are examples of RLs with spatially distributed feedback, where random local variations of the refractive index are introduced into the active region, obtaining an amplifying scattering medium.

A different approach has been proposed in the first works on lasers with non-resonant cavities [22,23], where a laser crystal was enclosed between a mirror and a scattering surface. We conceptualize that architecture as relying on a spatially *localized* feedback mechanism, since active medium and scattering elements are spatially separated. In those experiments, however, the typical spectrum of a coherent random laser, consisting of a multi mode emission with narrow spikes placed at random frequency positions, was not observed. It would be reported for the first time by Cao and colleagues, about thirty years later [6].

In this manuscript, we propose a RL with spatially localized feedback, where two scattering elements are placed at the ends of the optically pumped gain region. Multimode emission with randomly distributed frequency narrow peaks is detected emerging from the scattering media, which serve as feedback elements and output couplers. In this way, light travelling along the active medium is continuously amplified and the back-scattered radiation from the random media closes a feedback loop.

Random lasing emission is detected from scattering elements placed at large distance from each other. The entire device, with dimensions of  $2600 \times 650 \mu\text{m}^2$ , emits bright lasing radiation from its edges, where light is scattered off in all directions.

The manuscript is organized as follows: in Section 2, sample fabrication and experimental set-up are described. In Section 3, experimental results are described and in Section 4, conclusions are presented.

## 2. Fabrication of devices and experimental set-up

The DNA-CTMA complex is dissolved in ethanol and mixed with an ethanol-chloroform solution, like in [24]. Two kinds of devices are fabricated: with and without addition of scattering nano-particles of  $\text{TiO}_2$ .

Samples with scatterers are obtained as follows. Glass substrates are hydrophilized with a 20 minutes bath in chromic acid and a high concentration aqueous suspension of  $\text{TiO}_2$  nano-particles (Sigma-Aldrich 224227) is dropped onto the glass substrate. After water evaporation, regions of the deposited thick layer are selectively removed, obtaining two parallel “walls” of  $\text{TiO}_2$  particles, placed at 2.7 mm from each other with a clean region in between. The active polymer in liquid form is successively added and samples are dried into the oven at  $45^\circ\text{C}$  for 5 minutes.

In samples with no scattering elements, the  $\text{TiO}_2$  deposition step is not performed and the DCM-doped DNA-CTMA complex solution is directly dropped onto the glass substrate. The polymer is dried at  $45^\circ\text{C}$  for 5 minutes in the oven, obtaining a large patch of active material with circular shape with diameter of about 1 cm. Two parallel cuts at a distance of about 3 mm are performed onto the sample and the external regions of the film are ripped away from the substrate. In this way, we obtain a large stripe (with length of 1 cm) and width of 3 mm, with rough and irregularly shaped edges where the unwanted film was removed.

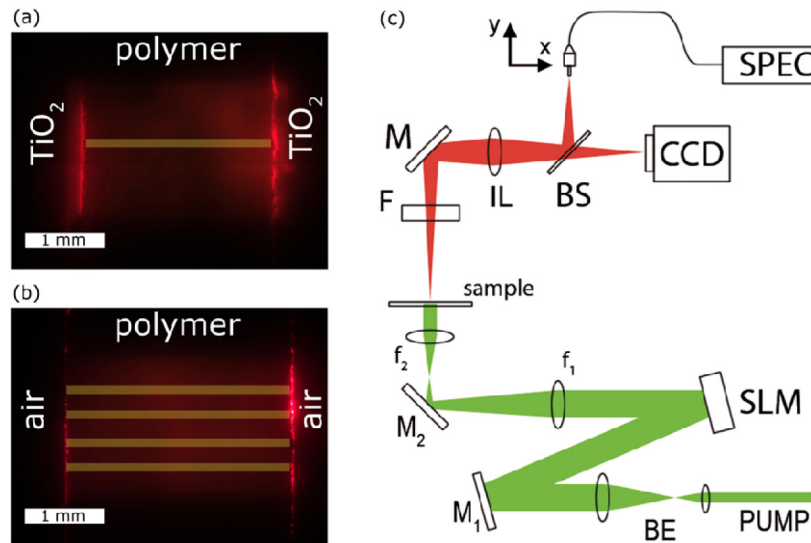


Fig. 1. Image of the sample with (a) and without (b)  $\text{TiO}_2$  particles when illuminated at low pump flux with full SLM screen. Rectangular regions are highlighted in yellow, corresponding to the excited regions in lasing experiments. (c) Experimental set-up, details are given in the text.

The set-up is schematically shown in Fig. 1(c). The pump source is a Q-switched Nd:YAG laser, frequency doubled at 532 nm (Litron NanoT250), emitting 10 ns pulses, at 10 Hz repetition rate. The pump transverse profile is shaped with a Spatial Light Modulator (SLM, Holoeye LCR-1080) operating in amplitude. The SLM liquid crystals screen is computer controlled and an arbitrary mask is sent to the device in the form of a matrix ( $1920 \times 1200$  elements) of black (non-reflective) and white (reflective) pixels. The amount of reflected light is controlled by imposing a variable gray level to the active pixels of the SLM.

The SLM image is reduced ( $\times 0.15$ ) with a pair of convex lenses with focal length  $f_1 = 20$  cm and  $f_2 = 3$  cm. Polarizing dichroic mirrors ( $M_1$ ,  $M_2$ ) are used in order to have linearly polarized light on the sample and a beam expander ( $\times 5$ ) is used to uniformly shine the SLM.

A large area of the sample ( $4.3 \text{ mm} \times 3.25 \text{ mm}$ ) is imaged (1:1) onto a CCD (Pixelink model PL-B776F) camera and on a connectorized fiber end ( $105 \mu\text{m}$  core diameter) with an imaging lens (IL, 15 cm focal length) and a beam splitter (BS). The pump light is stopped after the sample with an edgepass filter (F). The fiber core acts as a spatial filter which collects a circular area on the sample with the dimension of its core. Fiber collected light is sent to a 303-mm focal length spectrograph (SPEC, Andor, Shamrock 303) connected to a low-noise charge-coupled device array (Andor, iDus Spectroscopy CCD). Light is collected from different regions of the sample by positioning the fiber horizontally and vertically with two computer controlled translation stages. The collection points are mapped by using specific patterns imposed by the SLM: specifically, circular spots with diameter of  $100 \mu\text{m}$  are illuminated on the sample plane and the detected signal is maximized by moving the translation stages.

### 3. Results

We first characterize the Amplified Spontaneous Emission (ASE) from the polymer film by adapting to our set-up the variable stripe length technique [25]. A sample for ASE characterization is obtained after deposition of a drop of polymer in liquid form onto the glass substrate, the sample is dried and a very large circular area with diameter of about 1 cm and  $20 \mu\text{m}$  thickness is obtained.

A stripe shaped pump is projected onto the sample, with one end of the stripe located at the edge of the film. In this way, an ASE flux is established, which travels along the longitudinal direction of the stripe, and is scattered off the plane at the edge of the film (see inset of Fig. 2(a)). The pump fluence is set to  $20 \text{ pJ}/\mu\text{m}^2$ ; the length  $L$  of the stripe is varied between 0.4 mm and 4 mm and the emitted spectra are measured at each value of  $L$ . In Fig. 2(a), we show some spectra detected between  $L = 1.2 \text{ mm}$  and  $L = 4.0 \text{ mm}$ . A very broad spectrum with Full Width at Half Maximum (FWHM) of 80 nm and centered around 610 nm is measured for  $L = 1.2 \text{ mm}$  and smaller stripe lengths. As  $L$  is increased, the gain peak moves to 625 nm and the FWHM narrows down to 24 nm. This is attributed to the transition from the broad fluorescence spectrum to the narrower ASE emission, with the red shift due to solvatochromic effect of DCM dye in polymer [26].

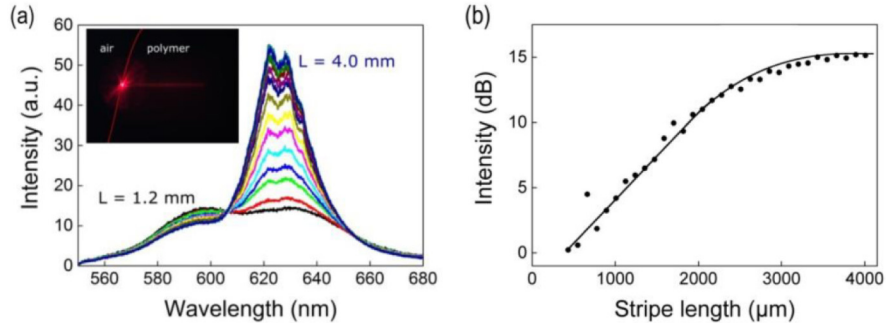


Fig. 2. (a) ASE spectra measured for different stripe lengths, curves obtained between 1.2 mm and 4.0 mm are shown. The inset shows the CCD image for measurement with  $L = 2.8 \text{ mm}$ . (b) Total measure intensity (full dots), obtained varying  $L$  from 0.4 mm to 4.0 mm, and fitted curve (solid line).

The measured spectra are integrated over the full spectral range of detection and the obtained total intensity is plotted as a function of the stripe length in Fig. 2(b). Intensity increases exponentially and saturates at about  $L = 2.3 \text{ mm}$ . We fitted the measured data as in [24, 25], obtaining a gain coefficient of  $15.4 \text{ cm}^{-1}$  in the linear region of measurements ( $L < 2.3 \text{ mm}$ ).

Experiments for lasing emission are performed on the two kinds of devices we fabricated: with and without addition of scattering particles of  $\text{TiO}_2$ . The active region of the samples is illuminated with a rectangular-shaped pump beam of width  $W = 50 \mu\text{m}$  and length  $L = 2.7 \text{ mm}$ , for samples with  $\text{TiO}_2$  and  $L = 3.0 \text{ mm}$  for sample without  $\text{TiO}_2$ , see Fig. 1(a) and 1(b). The pumped area is oriented in such a way that the longitudinal ends of the rectangular pump are placed close to the edges of the active area. The pump energy flux is  $20 \text{ pJ}/\mu\text{m}^2$ . Results are shown in Fig. 3(a)–3(d) and in Fig. 4(a)–4(d), for samples with  $\text{TiO}_2$  and without  $\text{TiO}_2$ , respectively.

In both cases, the same qualitative behavior is observed. Emission is detected at the ends of the pumped area from the scattering regions with local maxima and minima of intensity and spectra consisting of sharp peaks (with  $FWHM$  of about 0.3 nm) at random frequencies.

This is understood as due to the onset of lasing action in the entire structure, where the pumped area acts as amplifying, gain-guided, waveguide and the scattering regions as feedback elements and output couplers. Feedback is given by the backscattered light from the scattering regions that re-enters the pumped area and closes a feedback loop. Different intensity in same frequency peaks from left and right scatterers are attributed to direction and frequency dependent output coupling efficiency of each scattering region.

In samples with  $\text{TiO}_2$ , scattering is obtained due to the refractive index difference between the active polymer and  $\text{TiO}_2$  particles; in samples where no  $\text{TiO}_2$  was added, scattering is

obtained due to the refractive index difference between polymer and air at the rough interface produced by the manual film cutting.

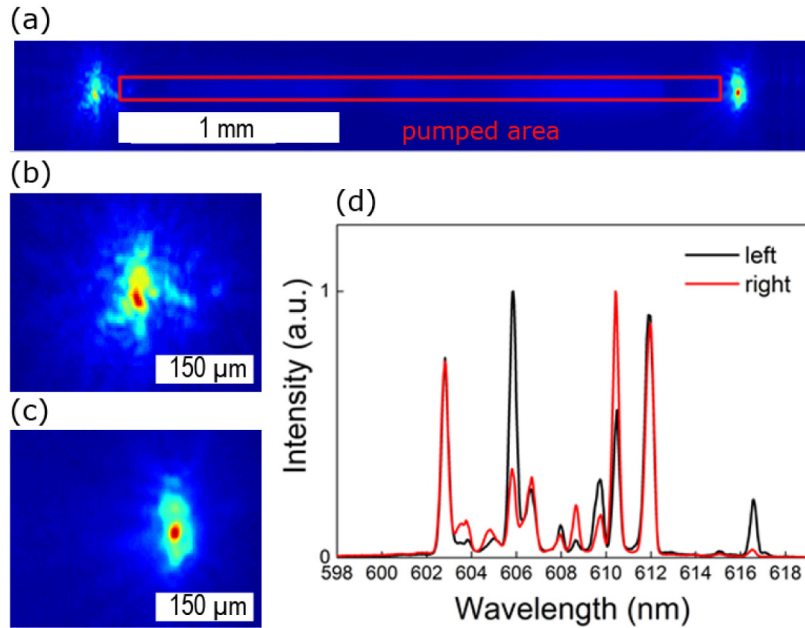


Fig. 3. Experimental results obtained with sampled with  $\text{TiO}_2$ : CCD image of the pumped region and emitting areas (a). Zoomed view of the left (b) and right (c) emitting region. Measured spectra (d) from left (black line) and right (red line) emitting region.

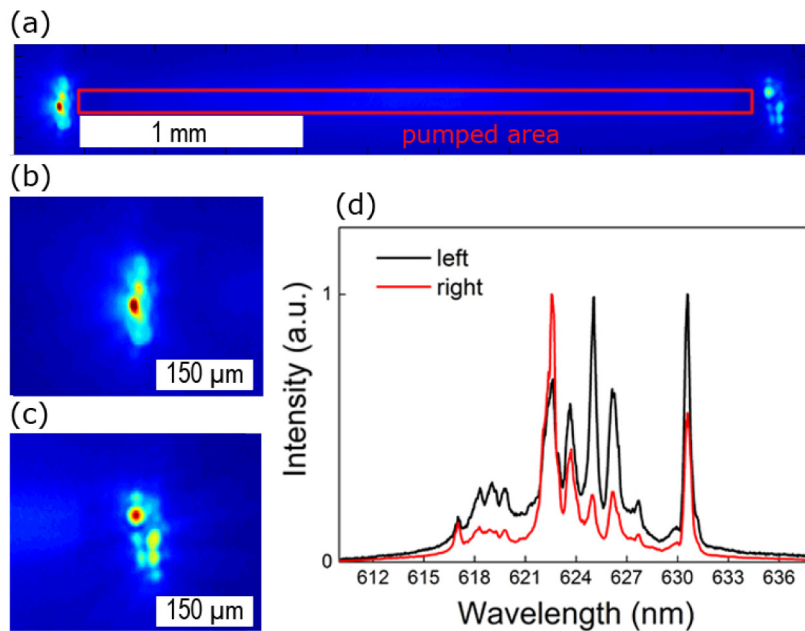


Fig. 4. Experimental results obtained with sampled without  $\text{TiO}_2$ : CCD image of the pumped region and emitting areas (a). Zoomed view of the left (b) and right (c) emitting region. Normalized measured spectra (d) from left (black line) and right (red line) emitting region.

The two structures shown here emit in neighboring spectral regions: between 600 nm and 618 nm for device with TiO<sub>2</sub> particles and between 615 nm and 633 nm for device without TiO<sub>2</sub> particles. This is attributed to the different thickness of the polymer films used (the ASE from thicker films is known [27, 28] to center at longer wavelengths). Devices without TiO<sub>2</sub> particles have been obtained from the film used in ASE characterization and their emission is centered around 625 nm, where the maximum peak of ASE has been measured, as shown in Fig. 2(a). The polymer film used in devices with TiO<sub>2</sub> particles is about 8 μm thick and the resulting emission is shifted more than 10 nm towards shorter wavelengths.

It's worth noting that no clear evidence of a distributed feedback along the pumped region of the polymer film is observed. In previous works on dye doped polymer film for random lasing without addition of scattering particles, as for example in [15], the surface roughness and randomly distributed imperfections of the films were used as scattering centers for random lasing. In our samples no emission in out-of-plane directions is detected from the pumped area, confirming that no scattering centers are found. In this context, the proposed structure is better described as relying on a spatially localized feedback, at variance with commonly diffused RLs based on a distributed feedback mechanism.

We estimated the threshold energy for both devices by varying the pump energy on the sample and integrating the measured spectra over the full range of detection. We obtained threshold values around 5 pJ/μm<sup>2</sup> for both kinds of devices and slope efficiencies in the order of 10<sup>-3</sup>. We remark that in our set-up, light is collected from the direction orthogonal to the device plane, thus we expect a low coupling efficiency which also depends on the optics used and the scattering elements.

Basically, the observed behavior is interpreted with an analogy with classical optical resonators, where specular mirrors are used instead of rough scattering surfaces. Radiation is trapped between scattering regions inside the active material where it is successively amplified at each round trip. Selection of narrow modes is in all likelihood due to the joint phase contribution of each scattering surface, which randomly back-scatters received radiation in all directions with different efficiency and phase delay. A full theoretical understanding of the presented results is out of the scope of the manuscript and we limit our interpretation to a qualitative level.

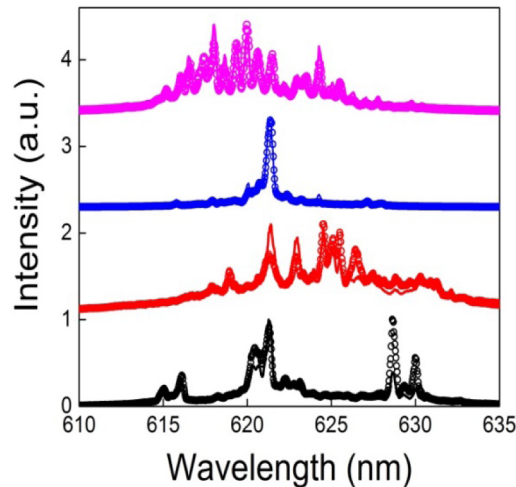


Fig. 5. Normalized measured spectra emitted from left (lines) and right (open circles) laser ends, pumping the polymer film without TiO<sub>2</sub> in different positions, highlighted in Fig. 1(b) with yellow rectangles.

We perform further experiments with the samples with no TiO<sub>2</sub>. Different regions of the sample with no TiO<sub>2</sub> are illuminated with  $L = 3$  mm,  $W = 50$  μm and  $E_p = 20$  pJ/μm<sup>2</sup>, see Fig.

1(b). By changing the position of the pumped area, *i. e.* using different regions of the rough scattering surfaces, the emitted spectrum changes strongly. As shown in Fig. 5, the number and spectral positions of modes vary randomly, for each position considered. This is attributed to different feedback contributions from regions of the polymer/air interface with different random roughness. However, for each position of the stripe the same spectral signature is always detected from both laser ends. We deduce that modes are selected by the joint contribution of the two opposite rough surfaces and each measurement corresponds to a different device, with its own spectrum. Notably the emission range that is obtained spans about 20 nm, suggesting that the whole available gain spectrum is used for lasing.

No clear spectral periodicity has been observed in any of the performed experiments. At variance with some RLs with distributed feedback architecture, where “closed loops” can be identified with power Fourier transform analysis [29], lasing modes in the proposed devices are understood as arising from the phase feedback of the back-scattering elements, *i.e.* TiO<sub>2</sub> particles or polymer/air defects.

The occurrence of sharp resonances is attributed to the spectrally uncorrelated phase contributions of the back-scattering media: a phase round trip condition is satisfied when a closed trajectory in the full resonator spans an integer number of wavelengths. For those frequencies at which the phase condition is satisfied, lasing modes are allowed to exist and grow.

We performed further experiments, keeping the position of the pump and the pump flux constant and varying the width of the stripe, until all four positions previously considered in Fig. 1(b) are covered by the pumped area. Results are shown in Fig. 6. Only spectra detected from the right end of the laser are shown, for clarity, as the same spectrum is detected at the left end. For large values of  $W$ , we verified that the same spectrum is emitted from any point of the scattering region.

As the pump width is increased, the detected spectrum changes randomly and different peaks appear at random frequency positions. The number of excited modes increases and the spectrum consists of a broad background and superimposed narrow spikes. For  $W > 1.0$  mm, narrow spikes are observed no more and a broad spectrum centered at 625 nm with *FWHM* of 10 nm, is measured.

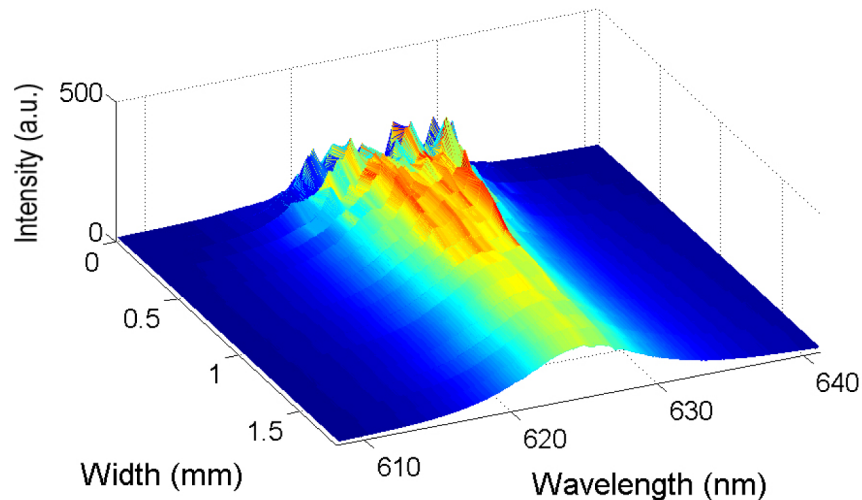


Fig. 6. Measured spectra as a function of  $W$ , with  $L = 3$  mm and  $E_p = 20$  pJ/ $\mu\text{m}^2$ . The width  $W$  is varied between 50  $\mu\text{m}$  and 1.8 mm.

The observed transition from multimode spiky spectrum to broad single peaked emission is attributed to the collective oscillation of a very large number of narrow modes, which

strongly interact and couple together, resulting in a mode-locked regime [9, 10]. Lasing modes change with increasing width due to their mutual interaction that through energy exchange establishes a gain competition that re-shapes the resulting emission spectrum that finally, for large widths adopts a broad single-peaked lineshape.

From a practical point of view, it would be advantageous to avoid the need for the SLM in obtaining resonant feedback random emission only through proper design of the device geometry. In this pursuit, by simply cutting a narrow stripe of the dye doped polymer film, we have been able to obtain resonant feedback random lasing by uniform illumination of the entire sample. The device is obtained with the same fabrication process described in Section 2. The width of the polymer stripe is imposed by the physical limitation of the manual process for film cutting, as stripes narrower than  $600\ \mu\text{m}$  are involuntary ripped away from the substrate. A device with dimensions of  $2.6\ \text{mm} \times 0.65\ \text{mm}$  is obtained and results are shown in Fig. 7. Emission spectra are measured from different points of the sample edges, labelled I through to VI in Fig. 7(a). The rough interface with air along the irregular edges of the film stripe serves as scattering element, similarly to experiments performed with the SLM. The measured spectra show narrow spikes at random frequencies, superimposed onto a broad background. Peak frequencies observed at distant points are the same indicating that the entire device is working as a single RL with very large area.

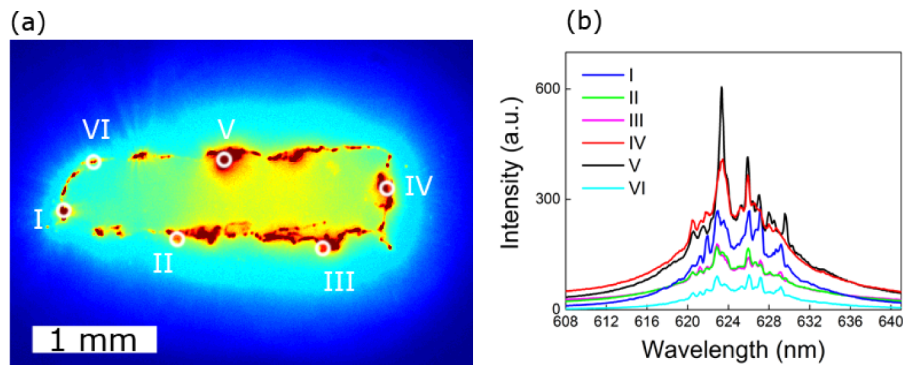


Fig. 7. Experiments performed with a uniformly pumped device with dimensions of  $2.6\ \text{mm} \times 0.65\ \text{mm}$  (a). Emission spectra detected from the devices edges at points labelled I-VI (b).

#### 4. Conclusions

A novel approach for obtaining random lasing action in disordered structures is proposed: we fabricated our devices by enclosing an active region, a DCM doped DNA-CTMA polymer film, between two rough scattering surfaces, where scattering centers are randomly positioned. The main difference with commonly used RLs, is that no distributed feedback inside the active material is imposed, the scattering regions being positioned at the edges of the pumped area. This architecture allowed us to detect the same spectral signature from two separated different random agglomerations of scatterers because the entire structure is working as a single optical oscillator where the scattering regions act as feedback elements and output couplers.

We first test this novel approach in two kinds of devices: one where scattering elements are  $\text{TiO}_2$  nano-particles and another where scattering centers are produced by the rough interface between active region and air. The same qualitative behavior, with clear evidence of random lasing with resonant feedback from the entire structure, is observed demonstrating the universality of the proposed architecture with spatially localized feedback.

We observed random lasing with resonant (narrow stripe pumping) and non-resonant (broad stripe pumping) spectral signatures, depending on the geometry of the pump beam.

In order to dispense with the beam shaping of the pump and simplify the whole set-up, we designed a device with optimized geometry, obtaining a large area RL with dimensions of 2.6 mm × 0.65 mm. The same laser modes (with FWHM = 0.3 nm) are detected on distant positions on the device edges. This demonstrates that the entire sample is acting as a single random oscillator with dimensions of several hundreds of micrometers, being a promising device for lighting, display and imaging applications.

### **Acknowledgments**

This work was partially funded by the Spanish Ministerio de Economía y Competitividad (MINECO) MAT2012-31659 (SAMAP) and Comunidad Autónoma de Madrid S2009/MIT-2740 (PHAMA\_2.0) projects.